

Research Article

Simulating the Performance of $\text{Al}_{0.3}\text{Ga}_{0.7}\text{As}/\text{InP}/\text{Ge}$ Multijunction Solar Cells under Variation of Spectral Irradiance and Temperature

Tony Sumaryada , **Siti Rohaeni**, **Nurlia Eka Damayanti**, **Heriyanto Syafutra**,
and **Hendradi Hardhienata** 

Theoretical Physics Division, Department of Physics, Bogor Agricultural University, Jl. Meranti, Kampus IPB Dramaga, Bogor 16680, Indonesia

Correspondence should be addressed to Tony Sumaryada; tsumaryada@ipb.ac.id

Received 30 August 2018; Revised 15 December 2018; Accepted 8 January 2019; Published 5 February 2019

Academic Editor: Jing-song Hong

Copyright © 2019 Tony Sumaryada et al. This is an open access article distributed under the Creative Commons Attribution License, which permits unrestricted use, distribution, and reproduction in any medium, provided the original work is properly cited.

The effect of spectral irradiance and temperature variation on the performance of the mechanically stacked $\text{Al}_{0.3}\text{Ga}_{0.7}\text{As}/\text{InP}/\text{Ge}$ multijunction solar cells was investigated using a simulation approach. The incoming and transmitted spectra of each subcell were simulated by using MATLAB codes, while PC1D software did the power-producing simulations. The incoming solar radiation on the first subcell was a multiplication of AM1.5d spectrum with the value of spectral irradiance multiplication factor (SIMF) 1, 5, 10, 50, 100, 150, and 200 suns. Each set of simulation was done at 25°C, 50°C, 75°C, and 100°C. The simulation results have shown a linear behavior of the open-circuit voltage and the efficiency of the solar cells upon variation of temperature, while the nonlinear response of the solar cells performance was obtained due to the change of SIMF. The simulation results also suggest that the spectral irradiance exposure at 100 suns and the operating temperature of 25°C give the highest efficiency.

1. Introduction

Over the last couple of decades, the progress on the renewable energy research has significantly increased, especially in the field of solar photovoltaics. Various types of solar cells such as silicon-based material, CIGS-based (copper indium gallium arsenide) material, and III-V-based chemical group have been intensively studied to produce a highly efficient solar cell. Some recorded achievements such as References [1–4] have decorated the global effort to find a better solar cell which is capable of producing clean and sustainable energy for a better future.

The combination of the III-V-based solar cells materials such as GaInP, AlGaAs, InP, and GaAs in the form of multijunction solar cells (MJSCs) and their exposure to the several hundreds multiplication of solar radiation had produced the efficiency rate up to 46% at 508 suns for the GaInP/GaAs/GaInAsP/GaInAs system [4]. Some new

experimental results and aspects in high-efficient solar cells such as the new design of a vertical epitaxial heterostructure architecture (which allows a high-efficient narrow band cells) [5, 6], the use of luminescent solar concentrators (LSCs) [7], or a six-junction solar cell [8] have also expanded our knowledge in solar cells research. Most of the experiments related to the high-efficient MJSC were done using a small specimen prototype, and their realization in the market and industrial scale is still far. More research related to multijunction solar cells are needed including the simulation and modeling aspect of MJSC performance under various conditions [9–13].

In a multijunction solar cell, several p-n junctions of semiconducting layers (or subcell) were put in order from top to bottom following the order of their bandgap energies. The first layer has the highest bandgap energy with the purpose to absorb the solar radiation in the small wavelength region, while the next layers with the smaller bandgap of

energy were set to absorb solar radiation in the longer wavelength regions. Theoretically, a higher efficiency rate can be obtained by putting more subcells in the solar cells [14].

Based on their fabrication technique, there are several types of MJSC such as the monolithically integrated solar cells and the mechanically stacked solar cells. In monolithic multijunction solar cells, the electric current matching, lattice matching, and tunnel junction between subcells become the main issues which limit the overall performance of MJSC. In the mechanically stacked multijunction solar cells, the abovementioned problems can be overcome by applying the separate load control for each subcell. The optical losses in the mechanically stacked multijunction solar cell are usually reduced by inserting an intermediate transparent and conductive layer such as ITO (indium titanium oxide) between two adjacent subcells.

There have been some experimental [15–18] and simulation studies [19–21] on the performance of multijunction solar cells under the variation of temperature and concentrated radiation, but to the best of author's knowledge, none of them discuss the $\text{Al}_{0.3}\text{Ga}_{0.7}\text{As}/\text{InP}/\text{Ge}$ solar cell. This paper is aimed at studying the performance of $\text{Al}_{0.3}\text{Ga}_{0.7}\text{As}/\text{InP}/\text{Ge}$ MJSC under the variation of spectral irradiance (produced by concentrators) and temperature through a simulation approach using the PC1D program [22]. The use of the PC1D program for simulating the effects mentioned above on MJSC, again to the best of author's knowledge, has never been found in the literature before. Hopefully, this study might help us in designing a robust, stable, and highly efficient solar cell in the future.

2. Methods

Three steps need to be done in this research. First, the preparation of the incoming spectrum; second, the calculation of the absorption coefficient and the transmitted radiation; and the last step is the power-producing simulation. The first two steps were done numerically by solving some related formulas using MATLAB while the next step was done using a freely available PC1D program [22]. All these steps must be done for each subcell.

The incident spectral irradiance on the first subcell for one sun radiation was taken from AM1.5d direct solar spectrum (ASTM G173-03), while the multiplied spectral irradiances (5, 10, 50, 100, 150, and 200 suns) were obtained by multiplying this spectrum with its corresponding amplification factor. The freely available AM1.5d data in the web have a drawback due to discontinuous steps in the wavelength. To overcome this problem and to gain a smooth AM1.5d spectral irradiance, we must first reconstruct the radiation spectrum by using a blackbody radiation formula in Equation (1) and determine the constant $b(\lambda)$, where $b(\lambda) = 1$ for blackbody radiation and $0 < b(\lambda) < 1$ for the actual spectral irradiance. The temperature of blackbody radiation was set to $T = 6000$ K. The spectral irradiance (intensity divided by wavelength) of blackbody radiation received by the earth's surface (terrestrial) is expressed as follows:

$$I_1(\lambda, T) = \frac{2\pi hc^2}{\lambda^5} \left(\frac{1}{\exp(b(\lambda) \cdot ((hc/\lambda)/(k_B \cdot T)))} \right) \cdot \left(\frac{r_{\text{sun}}}{R} \right)^2, \quad (1)$$

where r_{sun} is the radius of the sun, R is the distance between the center of the sun and the earth's surface, h is Planck's constant, and k_B is Boltzmann's constant. By integrating the whole spectrum using a trapezoid method and setting the intensity value to 989.9 W/m^2 (the total intensity of AM1.5d spectrum is the entire area under the $I(\lambda)$ versus λ curve), we can get the value of $b(\lambda)$ and reconstruct the smoothed AM1.5d spectrum using interpolation method.

The coefficient of absorption of each subcell was calculated using Equation (2) following the reference [23]:

$$\alpha(\lambda) = 5.5 \sqrt{(E(\lambda) - E_g)} + 1.5 \sqrt{E(\lambda) - (E_g + 0.1)} \mu\text{m}^{-1}, \quad (2)$$

where $\alpha(\lambda)$ is the coefficient absorption as a function of the wavelength, E_g is the bandgap energy of the corresponding subcell, and $E(\lambda)$ is the incoming photon energy at a particular wavelength.

The transmitted intensity to the next subcell I_{n+1} depends on the amount of the previous solar radiation I_n , the thickness of the previous subcell d_n , and the absorption coefficient of the previous subcell $\alpha_n(\lambda)$, which is as follows:

$$I_n(\lambda) = I_{n-1}(\lambda) \cdot e^{-\alpha_n(\lambda) \cdot d_n}, \quad n = 1, 2, 3 \text{ for triple-junction solar cells}, \quad (3)$$

where I_0 is the incoming spectral irradiance at the first subcell, I_1 is the incoming spectral irradiance at the second subcell, and I_2 is the incoming spectral irradiance at the third subcell. The thickness of the n th cell, d_n , was calculated using the PC1D program. Since this program can only simulate one layer at a time, several simulations must be performed, depending on the number of junctions involved. The incoming multiplied radiation is then calculated using the following equation:

$$I_{\text{mul}} = I_0 \cdot \text{SIMF}, \quad (4)$$

where I_{mul} is defined as the multiplied incoming spectral irradiance. The SIMF (spectral irradiance multiplication factor) was set to 1, 5, 10, 50, 100, 150, and 200 and has the unit of suns. For each set of simulation (at a specific value of SIMF and temperature), we simulated the electrical performance of the MJSC in the form of the short circuit current (I_{SC}), the open circuit voltage (V_{OC}), the output power of each subcell (P_n), and the total efficiency (η). The total efficiency of the mechanically stacked multijunction solar cells is then calculated using the following equation:

$$\eta = \left(\frac{P_1 + P_2 + P_3}{P_0} \right). \quad (5)$$

There are two types of MJSC simulation. First, the identical electric current model, and second, the non-identical electric current model [13]. In an identical current

model (a series connection of the subcells), the amount of current flowing in each subcell is set to be the same. The current in the last subcell will dictate the amount of current in the whole MJSC because the last subcell (in the bottom layer) receives the least amount of spectral irradiance and produces the smallest current, and as a consequence, the output and the total efficiency of the MJSC will be dragged down in this model. The nonidentical electric current model, such as the case of mechanically stacked multijunction solar cells, in contrast, will maximize the output power in each subcell and increase the total efficiency of the solar cells. This nonidentical current model can increase the total efficiency by a factor of 1.7 as reported in Reference [13]. If the current record of MJSC's efficiency is 45%, then the expected efficiency of the nonidentical current model can reach above 70%. This high value of solar cells efficiency under concentrated radiation has been theoretically predicted before, as can be found in Reference [24]. Although in reality, the nonidentical current model (harvesting the power from each subcell independently) seems unrealistic as compared to the identical current model, choosing this model does not change the intrinsic properties of MJSC in responding to the variation of temperature and incoming spectral irradiance. Note that this modeling can be considered as a toy model since some idealizations have been used here. The non-uniformity factors at the cell level which creates problems such as the occurrence of hotspots, the current mismatch between subcells, and the increase of resistive losses [25] were not taken into account in this paper.

3. Results and Discussions

The spectrum of incoming radiation was calculated using Equations (1) and (3). In Figure 1, the solar radiation spectrum at the temperature of 25°C and SIMF = 1 and 200 were chosen to represent the entire spectra. As the SIMF value increased, the maximum spectral irradiance and intensity received by the MJSC. The energy gap and the absorption coefficient of each subcell will limit the spectrum range of absorbed spectral irradiance following the cutoff wavelength of each junction ($\lambda_{\text{cutoff}} = h \cdot c / E_g$). Based on that cutoff wavelength, the absorbed spectrum of $\text{Al}_{0.3}\text{Ga}_{0.7}\text{As}$ was found within 280 nm to 685 nm range while for InP, within 598 to 841 nm and for Ge, within 872 to 1773 nm spectral range. Some overlapped regions between two adjacent subcells cannot be seen in Figure 1 due to overlapping colors.

The standard simulation at one sun spectral irradiance and the temperature of 25°C was used as a reference for other simulations as suggested in Reference [19]. Some parameters from the one sun simulation such as the thickness of the subcell, the value of p-doping and n-doping of each subcell, and the absorption spectrum range as shown in Table 1 will be used as reference values for the whole simulations performed in this research. For other simulations, the quick batch menu in the PC1D program was used to obtain the maximum total efficiency by varying the value of n-doping and p-doping based on this standard simulation (around $10^{20}/\text{cm}^3$ for n-doping and $10^{16}/\text{cm}^3$ for p-doping). The

thickness of each subcell in all simulations was kept constant following the values as shown in Table 1 ($2.778 \mu\text{m}$ for $\text{Al}_{0.3}\text{Ga}_{0.7}\text{As}$, $3.50 \mu\text{m}$ for InP, and $4.0 \mu\text{m}$ for Ge) since we only focus on the effect of spectral irradiance and temperature variation of MJSC.

The application of solar concentrator to MJSC not just affects the amount of radiation absorbed but also increases the temperature of the solar cells. In this simulation, the performance of MJSC was evaluated at 25°C, 50°C, 75°C, and 100°C. The increasing temperature received by MJSC will reduce its performance as shown in Figure 2(a), where the total efficiency drops with the rate of around $-0.10\%/^{\circ}\text{C}$. The linear dependence (with the negative slope) of the overall efficiency to temperature is similar to the monotonic behavior of a traditional monolithic MJSC, where a lattice mismatch between two adjacent subcells will dissipate the transmitted power and reduce the solar cell performance [26–28]. The same behavior was also found in open-circuit voltage (V_{oc}) of each subcell, where V_{oc} linearly depends (with the negative slope) on temperature. A higher temperature will produce a more substantial lattice mismatch that eventually reduces V_{oc} and the output power. The V_{oc} drop and power loss might also come from the overlapping of the absorption region of two adjacent subcells which reduces the amount of energy (photon) absorbed in the next subcell. The linear behavior of V_{oc} to temperature for the three subcells is shown in Figures 2(b)–2(d). The negative slope of the plots indicated the coefficient temperature of V_{oc} for each subcell in Figures 2(b)–2(d) and was found to be around $-1.0 \text{ mV}/^{\circ}\text{C}$ which is in a reasonable agreement with the results of other III-V-based MJSC [15, 17, 18, 29, 30].

Multiplication of spectral irradiance will accumulate a significant amount of photon (and energy) received by MJSC. Depending on the electronic structure of each material, there is a limit of the number of absorbed photons by each subcell. The excess unabsorbed photons will generate the heat and raise the temperature of the subcell to the point which potentially could melt the subcell itself. By assuming that MJSC in this simulation equipped with a cooling system that keeps the temperature of the subcell to be 25°C, 50°C, 75°C, and 100°C, we expect to only see the MJSC's response to the variation of spectral irradiance and intensity.

The total efficiency of the MJSC increases nonlinearly (logarithmically) as a function of SIMF and reaches a peak at around 100 suns solar intensity, before decreasing and tends to saturate at a particular value as seen in Figure 3(a). The same behavior is also found by other researchers in the III-V-based-MJSC [15, 17, 18, 31, 32]. The logarithmic behavior of this MJSC is in agreement with the existing model from Nishioka et al. [33] which use a one-diode approximation model. The amount of total efficiency enhancement within 1 to 100 suns and 100 to 200 suns spectral irradiance are shown in Table 2. It was found that from 1 to 100 suns, the total efficiency of MJSC increased by 22% on average, while for 100 to 200 suns, the total efficiency dropped by 5% on average. The application of solar concentrator to raise the spectral irradiance exceeding the peak of efficiency is not necessary since above the peak limit, the total efficiency will

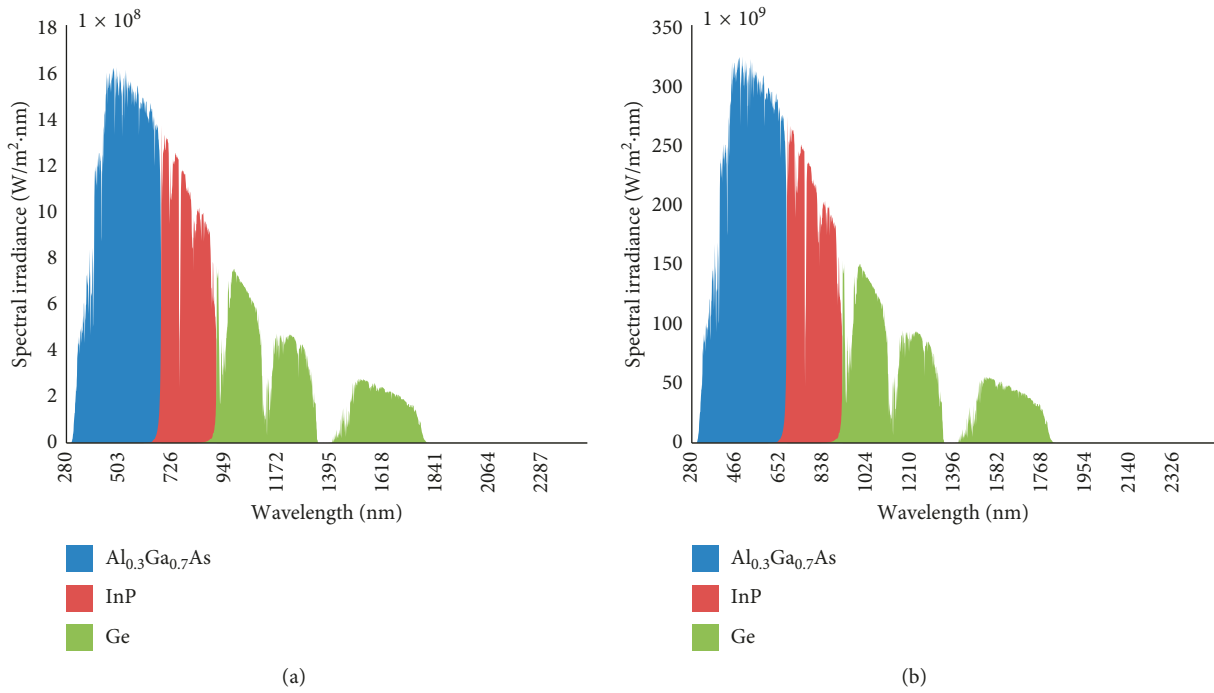


FIGURE 1: The incoming AM1.5d spectrum and the range of absorption of each subcell for (a) SIMF = 1 (1 sun) and (b) SIMF = 200 (200 suns).

TABLE 1: The input parameters for the standard simulation (at one sun spectral irradiance and the temperature of 25°C).

| Subcell | Energy gap (eV) | Thickness (μm) | p-Doping (cm^{-3}) | n-Doping (cm^{-3}) | Absorption spectrum (nm) |
|---|-----------------|-----------------------------|-------------------------------|-------------------------------|--------------------------|
| $\text{Al}_{0.3}\text{Ga}_{0.7}\text{As}$ | 1.817 | 2.778 | 1.0×10^{16} | 1.0×10^{20} | 280–685 |
| InP | 1.350 | 3.500 | 1.0×10^{16} | 1.11×10^{17} | 598–841 |
| Ge | 0.664 | 4.000 | 1.0×10^{16} | 1.12×10^{17} | 872–1773 |

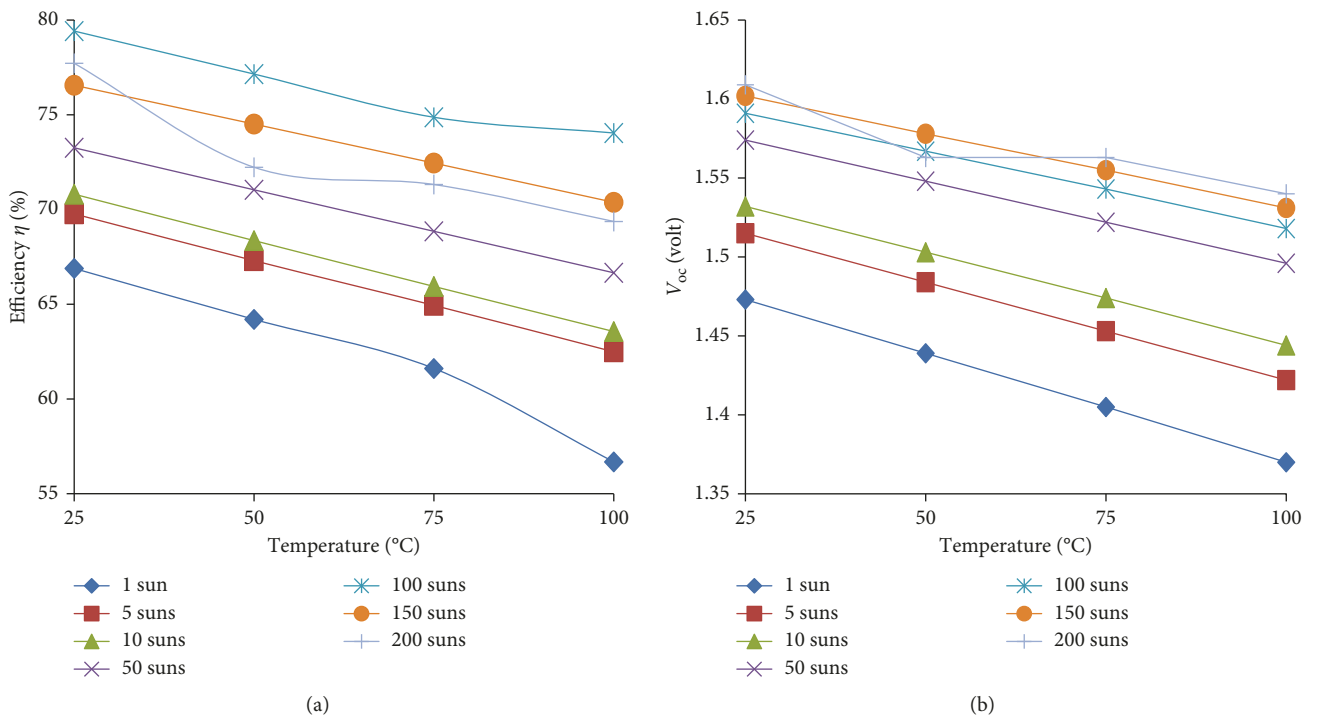


FIGURE 2: Continued.

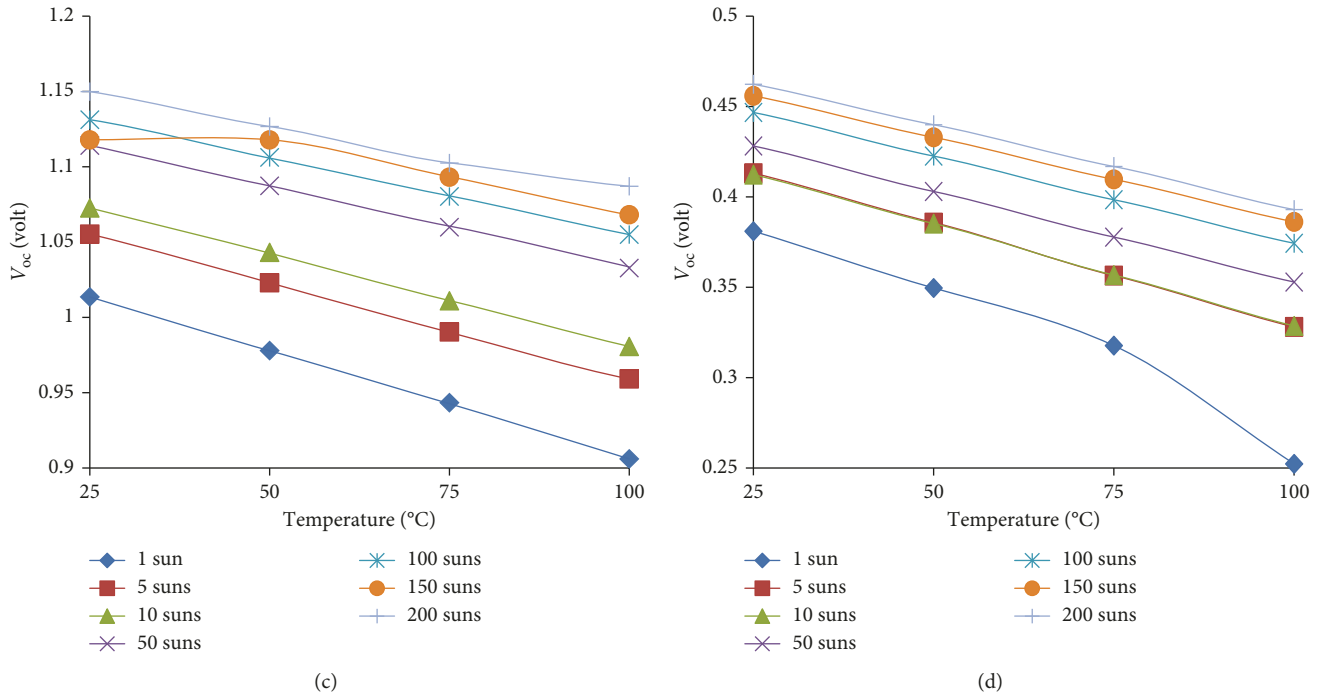


FIGURE 2: The effect of temperatures on (a) the efficiency of $Al_{0.3}Ga_{0.7}As/InP/Ge$ multijunction solar cells. The effect of temperature on the open-circuit voltage of (b) the first subcell $Al_{0.3}Ga_{0.7}As$, (c) the second subcell InP , and (d) the third subcell Ge .

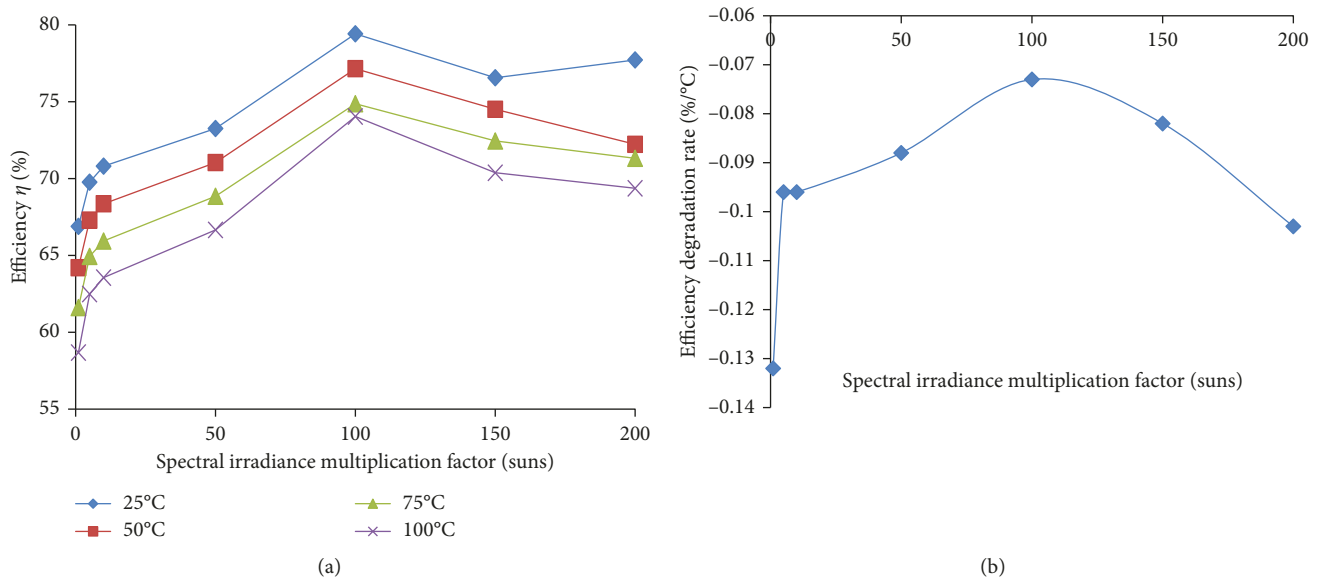


FIGURE 3: The effect of spectral irradiance multiplication on (a) the total efficiency of solar cells and (b) the efficiency degradation rate of solar cells.

TABLE 2: The efficiency enhancement at various temperatures and SIMF's ranges.

| Temperature (°C) | Efficiency enhancement within 1 to 100 suns of SIMF's range (%) | Efficiency enhancement within 100 to 200 suns of SIMF's range (%) |
|------------------|---|---|
| 25 | 18.73 | -2.14 |
| 50 | 20.17 | -6.37 |
| 75 | 21.52 | -4.74 |
| 100 | 30.63 | -6.31 |

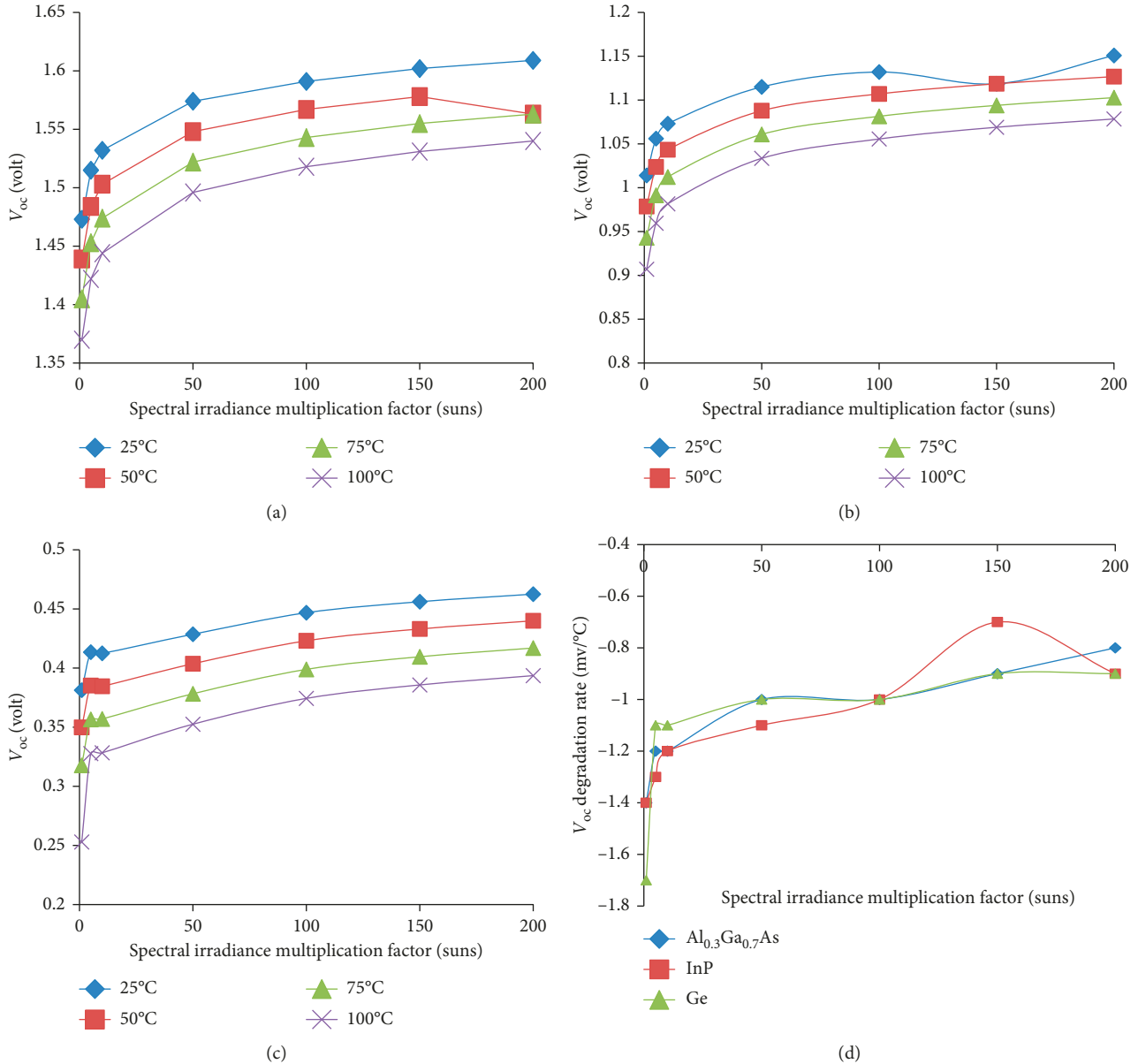


FIGURE 4: The effect of spectral irradiance multiplication to the open-circuit voltage (V_{oc}) of (a) the first subcell $Al_{0.3}Ga_{0.7}As$, (b) the second subcell InP, and (c) the third subcell Ge. The degradation rate of V_{oc} for each subcell is shown in (d).

slowly decrease and saturate to a particular value. In our simulations, the peak of efficiency was reached at 100 suns, so increasing the spectral irradiance above 100 suns economically is not feasible and even reduces the total efficiency and performance of $Al_{0.3}Ga_{0.7}As/InP/Ge$ solar cells.

The nonlinear behavior of MJSC to SIMF variation is also reflected in the degradation rate of solar cells efficiency as seen in Figure 3(b). The degradation rate of MJSC decreases from $-0.13\%/^{\circ}C$ to $-0.07\%/^{\circ}C$ as the SIMF increases from 1 to 100 suns before increasing again to $-0.10\%/^{\circ}C$ at 200 suns. Those results are in the reasonable agreement with the one found in another type of III-V-based MJSC which is around $-0.15\%/^{\circ}C$ to $-0.10\%/^{\circ}C$ [19].

As shown in Figure 3(a), the highest efficiency is obtained at 100 suns and 25°C, but keeping the temperature of

the MJSC at 25°C will also increase the operational cost due to the usage of additional cooling system instruments such as active cooling, passive cooling, and spray cooling or utilizing a phase change material [34]. To minimize this additional cost, a higher operational temperature ($T > 25^{\circ}C$) might be used at the expense of a slightly lower MJSC efficiency. Further studies to clarify this situation are still needed to be done in the future.

The open-circuit voltage of each subcell as a function of SIMF is shown in Figures 4(a)–4(c). As the value of SIMF increases, the amount of V_{oc} also increases before saturating to a particular point at the extreme SIMF value. Each subcell tends to have a similar response to SIMF as shown by the curve pattern which is almost identical in Figures 4(a)–4(c). The increasing temperature to 75°C reduces V_{oc} in the first

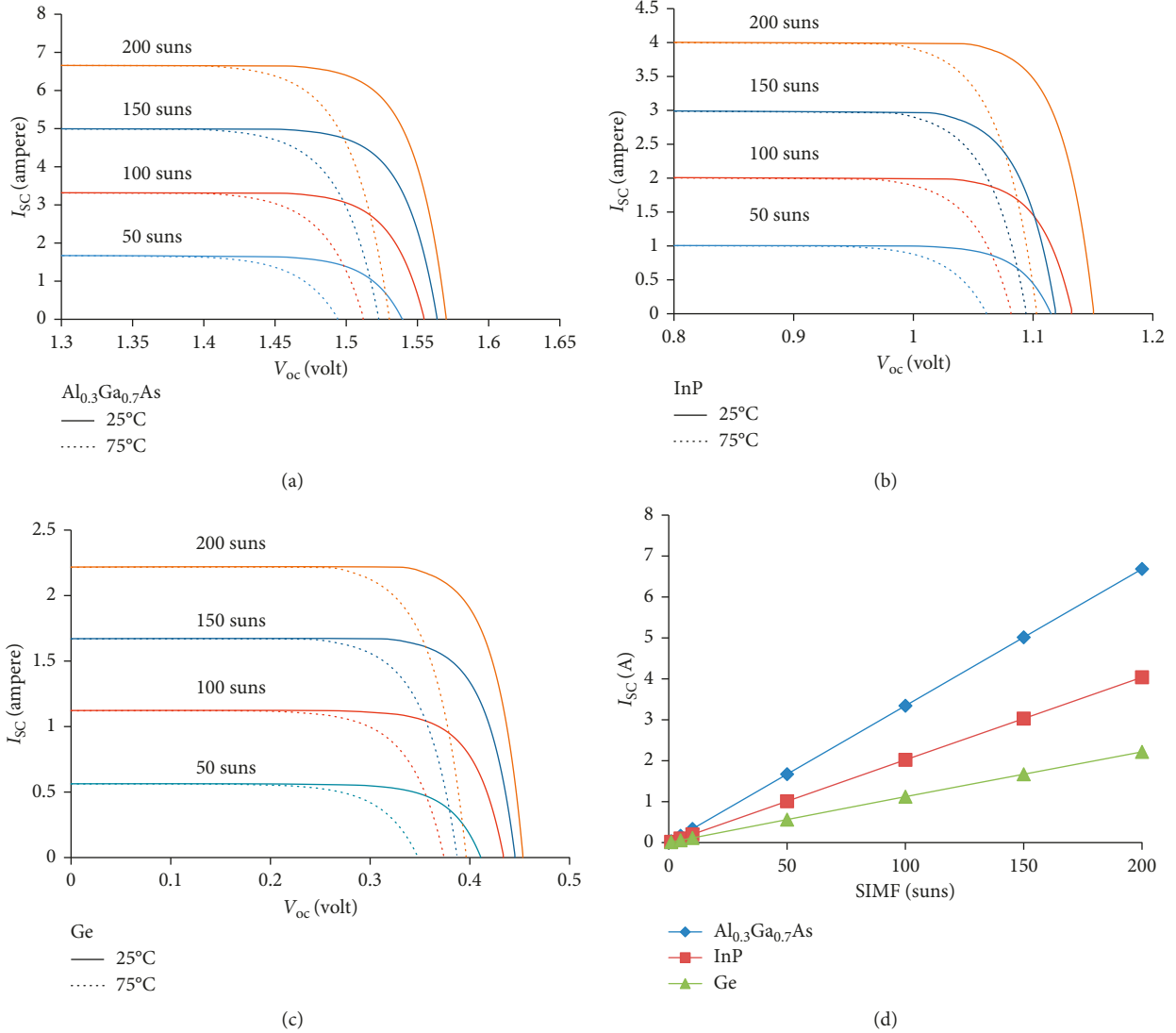


FIGURE 5: The comparison of I - V profile at 25°C (solid line) and 75°C (dotted line) and various SIMFs for (a) $Al_{0.3}Ga_{0.7}As$, (b) InP, and (c) Ge and (d) the short circuit current, I_{SC} , at various SIMFs.

subcell ($Al_{0.3}Ga_{0.7}As$) by 69 mV while in the second subcell (InP) by 72 mV and in the third subcell (Ge) by 69 mV. The variation of SIMF also shows no significant change in the value of V_{oc} degradation rate (coefficient temperature of V_{oc}) in all subcells as shown in Figure 4(d). The variation of the coefficient temperature of V_{oc} in the first subcell is only 0.6 mV and relatively small as compared to the maximum V_{oc} in the first subcell which is 1.61 V (about 0.04% variation of V_{oc} for each degree Celsius). For the second subcell, the variation of V_{oc} is only 0.05%/°C and for the third subcell 0.20%/°C. The application of spectral irradiance multiplication has demonstrated a reduction of subcell's sensitivity to the temperature as indicated by a roughly similar trend of curves in Figure 4(d). A similar conclusion was also reported in Reference [19].

The current-voltage (I - V) characteristic of each subcell at 25°C and 75°C and various SIMFs (50, 100, 150, and 200 suns) are shown in Figures 5(a)–5(c). The temperatures of

25°C and 75°C were selected to represent the effect of increasing temperature to the I - V characteristic of each subcell. We have excluded the I - V curve for 1, 5, and 10 suns in Figure 5 since the currents for those SIMFs were too small as compared to other SIMFs values. The detail data for all SIMFs are shown in Table 3. The short circuit current I_{SC} of each subcell depends linearly on the SIMF as seen in Figure 5(d). The increasing rates of I_{SC} for each subcell (as indicated by the slope of plots in Figure 5(d)) were found to be 33.0 mA/sun for $Al_{0.3}Ga_{0.7}As$ /InP/Ge, 20.0 mA/sun for InP, and 11.0 mA/sun for Ge. These results were expected, as more electric current produced by the increasing number of photon absorbed at high SIMF value. In general, Figure 5 describes that the rising temperature will reduce the open voltage (V_{oc}) of the subcell, while the increasing SIMF value will linearly increase the short circuit current (I_{SC}) of the subcell. Similar features were also found experimentally in Reference [18].

TABLE 3: The I - V performances of each subcell at various SIMFs at the temperatures of 25°C and 75°C.

| Subcell | SIMF (suns) | I_{SC} (A) | V_{oc} at 25°C (Volt) | V_{oc} at 75°C (Volt) |
|--|-------------|--------------|-------------------------|-------------------------|
| Al _{0.3} Ga _{0.7} As | 1 | 0.033 | 1.473 | 1.404 |
| | 5 | 0.167 | 1.510 | 1.453 |
| | 10 | 0.334 | 1.532 | 1.473 |
| | 50 | 1.671 | 1.574 | 1.521 |
| | 100 | 3.343 | 1.591 | 1.542 |
| | 150 | 5.015 | 1.601 | 1.554 |
| | 200 | 6.686 | 1.609 | 1.563 |
| InP | 1 | 0.020 | 1.014 | 0.943 |
| | 5 | 0.101 | 1.056 | 0.991 |
| | 10 | 0.202 | 1.073 | 1.012 |
| | 50 | 1.010 | 1.115 | 1.061 |
| | 100 | 2.022 | 1.132 | 1.081 |
| | 150 | 3.029 | 1.119 | 1.094 |
| | 200 | 4.038 | 1.150 | 1.103 |
| Ge | 1 | 0.011 | 0.381 | 0.318 |
| | 5 | 0.056 | 0.413 | 0.356 |
| | 10 | 0.113 | 0.412 | 0.357 |
| | 50 | 0.563 | 0.429 | 0.378 |
| | 100 | 1.122 | 0.447 | 0.399 |
| | 150 | 1.670 | 0.456 | 0.409 |
| | 200 | 2.217 | 0.463 | 0.417 |

4. Summary

We have simulated the performance of Al_{0.3}Ga_{0.7}As/InP/Ge multijunction solar cells under variation of spectral irradiance and temperature with a reasonable agreement of result as compared to other research studies on III-V-based MJSC (experimental and simulation). The multijunction solar cells have shown a linear response (with a negative slope) to V_{oc} and total efficiency to the temperature and a nonlinear (logarithmic) response to the multiplication of spectral irradiance (SIMF). The application of spectral irradiance multiplication has also demonstrated a reduction of subcell's sensitivity to the temperature. The nonlinear behavior of V_{oc} and total efficiency to SIMF is in agreement with the one-diode approximation model. Based on the material parameter assumptions used here, which in some cases might be favorable compared to experimentally achievable results, we find that illumination of Al_{0.3}Ga_{0.7}As/InP/Ge multijunction solar cells at 100 suns and 25°C gives the highest solar cell efficiency.

Data Availability

The simulation data are available upon request to the corresponding author.

Conflicts of Interest

The authors declare that they have no conflicts of interest.

Acknowledgments

The authors express their gratitude to Direktorat Riset dan Pengabdian Masyarakat, the Ministry of Research, Technology

and Higher Education of the Republic of Indonesia for funding this research through PUPT scheme contract no. 011/SP2H/LT/DRPM/IV/2017.

References

- [1] K. Masuko, M. Shigematsu, T. Hashiguchi et al., "Achievement of more than 25% conversion efficiency with crystalline silicon heterojunction solar cell," *IEEE Journal of Photovoltaics*, vol. 4, no. 6, pp. 1433–1435, 2014.
- [2] P. Jackson, D. Hariskos, E. Lotter et al., "New world record efficiency for Cu(In,Ga)Se₂ thin-film solar cells beyond 20%," *Progress in Photovoltaics: Research and Applications*, vol. 19, no. 7, pp. 894–897, 2011.
- [3] H. Zhou, Q. Chen, G. Li et al., "Interface engineering of highly efficient perovskite solar cells," *Science*, vol. 345, no. 6196, pp. 542–546, 2014.
- [4] F. Dimroth, T. N. D. Tibbits, M. Niemeier et al., "Four-junction wafer-bonded concentrator solar cells," *IEEE Journal of Photovoltaics*, vol. 6, no. 1, pp. 343–349, 2016.
- [5] S. Fafard, M. C. A. York, F. Proulx et al., "Ultrahigh efficiencies in vertical epitaxial heterostructure architectures," *Applied Physics Letters*, vol. 108, no. 7, article 071101, 2016.
- [6] M. C. A. York, A. Mailhot, A. Boucherif, R. Arès, V. Aimez, and S. Fafard, "Challenges and strategies for implementing the vertical epitaxial heterostructure architecture (VEHSA) design for concentrated photovoltaic applications," *Solar Energy Materials and Solar Cells*, vol. 181, pp. 46–52, 2018.
- [7] D. R. Needell, O. Ilic, C. R. Bukowsky et al., "Design criteria for micro-optical tandem luminescent solar concentrators," *IEEE Journal of Photovoltaics*, vol. 8, no. 6, pp. 1560–1567, 2018.
- [8] J. F. Geisz, M. A. Steiner, N. Jain et al., "Building a six-junction inverted metamorphic concentrator solar cell," *IEEE Journal of Photovoltaics*, vol. 8, no. 2, pp. 626–632, 2018.
- [9] R. R. King, D. C. Law, K. M. Edmondson et al., "40% efficient metamorphic GaInP/GaInAs/Ge multijunction solar cells," *Applied Physics Letters*, vol. 90, no. 18, article 183516, 2007.
- [10] M. Yamaguchi, K. I. Nishimura, T. Sasaki et al., "Novel materials for high-efficiency III-V multi-junction solar cells," *Solar Energy*, vol. 82, no. 2, pp. 173–180, 2008.
- [11] M. Yamaguchi, T. Takamoto, K. Araki, and N. Ekins-Daukes, "Multi-junction III-V solar cells: current status and future potential," *Solar Energy*, vol. 79, no. 1, pp. 78–85, 2005.
- [12] F. Dimroth, "High-efficiency solar cells from III-V compound semiconductors," *Physica Status Solidi (c)*, vol. 3, no. 3, pp. 373–379, 2006.
- [13] T. Sumaryada, R. Sobirin, and H. Syafutra, "Ideal simulation of Al_{0.3}Ga_{0.7}As/InP/Ge multijunction solar cells," *AIP Conference Proceedings*, vol. 1554, p. 162, 2013.
- [14] I. Tobias and A. Luque, "Ideal efficiency of monolithic, series-connected multijunction solar cells," *Progress in Photovoltaics: Research and Applications*, vol. 10, no. 5, pp. 323–329, 2002.
- [15] R. R. King, D. C. Law, K. M. Edmondson et al., "Advances in high-efficiency III-V multijunction solar cells," *Advances in Optoelectronics*, vol. 2007, Article ID 29523, 8 pages, 2007.
- [16] R. R. King, C. M. Fetzer, D. C. Law et al., "Advanced III-V multijunction cells for space," in *Proceedings of 2006 IEEE 4th World Conference on Photovoltaic Energy, WCPEC-4*, vol. 4, pp. 1757–1762, Waikoloa, HI, USA, May 2007.
- [17] H. Cotal, C. Fetzer, J. Boisvert et al., "III-V multijunction solar cells for concentrating photovoltaics," *Energy and Environmental Science*, vol. 2, no. 2, pp. 174–192, 2009.

- [18] H. Helmers, M. Schachtner, and A. W. Bett, "Influence of temperature and irradiance on triple-junction solar subcells," *Solar Energy Materials and Solar Cells*, vol. 116, pp. 144–152, 2013.
- [19] G. Siefert and A. W. Bett, "Analysis of temperature coefficients for III-V multi-junction concentrator cells," *Progress in Photovoltaics: Research and Applications*, vol. 22, no. 5, pp. 515–524, 2012.
- [20] A. Braun, E. A. Katz, and J. M. Gordon, "Basic aspects of the temperature coefficients of concentrator solar cell performance parameters," *Progress in Photovoltaics: Research and Applications*, vol. 21, no. 5, pp. 1087–1094, 2013.
- [21] E. F. Fernández, G. Siefert, F. Almonacid, A. J. G. Loureiro, and P. Pérez-Higueras, "A two subcell equivalent solar cell model for III-V triple junction solar cells under spectrum and temperature variations," *Solar Energy*, vol. 92, pp. 221–229, 2013.
- [22] P. A. Basore and D. A. Clugston, "PC1D version 4 for windows: from analysis to design," in *Proceedings of 25th IEEE Photovoltaic Specialists Conference-1996*, pp. 377–381, Washington, DC, USA, May 1996.
- [23] A. Luque and S. Hegedus, *Handbook of Photovoltaic Science and Engineering*, John Wiley & Sons, Hoboken, NJ, USA, 2011.
- [24] E. F. Fernández, A. J. García-Loureiro, and G. P. Smestad, "Multijunction concentrator solar cells: analysis and fundamentals," *High Concentrator Photovoltaics*, vol. 190, pp. 9–37, 2015.
- [25] O. Richard, V. Aimez, R. Arès, S. Fafard, and A. Jaouad, "Simulation of through-cell vias contacts under non-uniform concentrated light profiles," *Solar Energy Materials and Solar Cells*, vol. 188, pp. 241–248, 2018.
- [26] A. Aho, R. Isoaho, A. Tukiainen et al., "Temperature coefficients for GaInP/GaAs/GaInNAsSb solar cells," *AIP Conference Proceedings*, vol. 1679, article 050001, 2015.
- [27] A. Ben Or and J. Appelbaum, "Dependence of multi-junction solar cells parameters on concentration and temperature," *Solar Energy Materials and Solar Cells*, vol. 130, pp. 234–240, 2014.
- [28] T. Sumaryada, N. E. Damayanti, S. Rohaeni et al., "Modeling the thermal response of $\text{Al}_{0.3}\text{Ga}_{0.7}\text{As}/\text{GaAs}/\text{Ge}$ multijunction solar cells," *Journal of Physics: Conference Series*, vol. 877, article 012030, 2017.
- [29] F. Dimroth, M. Grave, P. Beutel et al., "Wafer bonded four-junction GaInP/GaAs//GaInAsP/GaInAs concentrator solar cells with 44.7% efficiency," *Progress in Photovoltaics: Research and Applications*, vol. 22, no. 3, pp. 277–282, 2014.
- [30] R. R. King, D. C. Law, K. M. Edmondson et al., "Metamorphic and lattice-matched solar cells under concentration," in *Proceedings of 2006 IEEE 4th World Conference on Photovoltaic Energy, WCPEC-4*, vol. 1, pp. 760–763, Waikoloa, HI, USA, May 2007.
- [31] Z. Wang, H. Zhang, W. Zhao, Z. Zhou, and M. Chen, "The effect of concentrated light intensity on temperature coefficient of the InGaP/InGaAs/Ge triple-junction solar cell," *Open Fuels and Energy Science Journal*, vol. 8, pp. 106–111, 2015.
- [32] D. Derkacs, R. Jones-Albertus, F. Suarez, and O. Fidaner, "Lattice-matched multijunction solar cells employing a 1 eV GaInNAsSb bottom cell," *Journal of Photonics for Energy*, vol. 2, no. 1, article 021805-1, 2012.
- [33] K. Nishioka, T. Takamoto, T. Agui, M. Kaneiwa, Y. Uraoka, and T. Fuyuki, "Annual output estimation of concentrator photovoltaic systems using high-efficiency InGaP/InGaAs/Ge triple-junction solar cells based on experimental solar cell's characteristics and field-test meteorological data," *Solar Energy Materials and Solar Cells*, vol. 90, no. 1, pp. 57–67, 2006.
- [34] S. Sargunanathan, A. Elango, and S. T. Mohideen, "Performance enhancement of solar photovoltaic cells using effective cooling methods: a review," *Renewable and Sustainable Energy Reviews*, vol. 64, pp. 382–393, 2016.



Hindawi

Submit your manuscripts at
www.hindawi.com

